Investigation of the Structural Conformation of Biphenyl by Solid State ^{13}C NMR and Quantum Chemical NMR Shift Calculations

Dewey H. Barich,[†] Ronald J. Pugmire,[‡] and David M. Grant*,[†]

Departments of Chemistry and of Chemical and Fuels Engineering, University of Utah, Salt Lake City, Utah 84112

Robbie J. Iuliucci

Department of Chemistry, Washington and Jefferson College, Washington, Pennsylvania 15301

Received: November 28, 2000; In Final Form: April 16, 2001

The principal values of the ^{13}C chemical-shift tensor (CST) for biphenyl have been determined with the FIREMAT experiment. The internal dihedral angle between the benzene rings in biphenyl is estimated to fall between 10 and 20° on the basis of quantum mechanical calculations of the CST principal values. A composite model of motion in the system, with contributions both from internal jumping between enantiomeric structures and from overall molecular librations, yields the smallest variance between predicted and measured values for an internal twist angle of 15° between the rings and a mean libration angle of ±12° from the most favored molecular orientation. The composite model is clearly preferred to a motionless model (with >98% probability) and is also preferred over either of the isolated contributing dynamics, i.e., only libration or only internal jumping.

Introduction

The structure of biphenyl varies depending upon the material's phase. The primary structural difference is the twist angle between the two phenyl rings. For example, biphenyl has a twist angle of 44.4° in the gas phase.[1,2] In solution estimates range from 19° to 32° for the parent molecule in various media.[3,4] This inter-ring angle also changes as a function of ortho substitution. The angle may be even smaller in the solid because crystal packing forces could contribute to the torsion barrier of the two phenyl rings relative to one another.

High-temperature X-ray studies[5−12] (110−298 K) report a *planar structure* with space group $P2_1/a$ in which the midpoint of the phenyl−phenyl linkage lies at a crystallographic inversion center. While many of the early X-ray studies assumed a rigid planar model, Charbonneau and Delugeard[12] proposed in 1977 that the unusually large mean libration vibration (λ_{av}^2 = 109.17° ^{2}) around the long molecular axis suggests that the observed *planar structure* is in fact the *statistical average* over two equivalent twisted conformations about the phenyl−phenyl linkage creating a double-well potential. Heat capacity measurements by Atake et al.[13] have shown that the crystal experiences a displacive phase transition near 40 K. At 22 K[14] the biphenyl crystal structure has been determined to belong to space group *Pa*. In both of these low temperature structures the two connected rings are permanently twisted from one another by approximately 10°, destroying the aforementioned crystallographic inversion center observed at room temperature. This loss of an effective inversion center doubles the unit cell axis length associated with the long axis of biphenyl. Similar features are observed[15] for other polyphenyls such as *p*-terphenyl[16,17] and *p*-quaterphenyl.[18,19]

The chemical-shift tensors (CST) of polycyclic aromatic compounds have received considerable attention in the past decade.[20−24] Most of these molecules are static in the crystal structure, as they exhibit rigid molecular structures. Biphenyl is unusual in that the phenyl−phenyl linkage has a rotational degree of freedom not present in most polycyclic aromatic compounds. Regrettably, NMR cannot observe translation effects where no change in orientation with respect to the magnetic field occurs. Hence, the displacive phase transitions observed at very low temperatures cannot be addressed in this work. However, CSTs provide the opportunity to investigate rotational modes that occur in the crystal system independently of the displacive effects. The measured CST principal values reported here demonstrate that the room-temperature crystal structure of biphenyl indeed undergoes constrained rotational averaging about the phenyl−phenyl linkage. Quantum chemical predictions of the full CST (both principal values and orientations) provide the means to demonstrate the importance of rotational motion. The experimental tensor orientations and averages derived from reliable full tensor calculations properly considered with the dynamical models are discussed below. The tensor averaging of two mirror-image twisted biphenyls eliminates some off-diagonal elements and changes the principal values of the final, effective tensor.

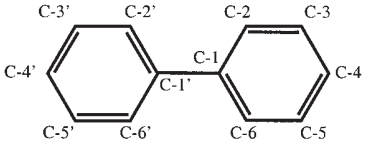

Because of the small range of values for the isotropic chemical shifts of the protonated carbons (125.5−129.8 ppm) and the large line widths (ca. 2 ppm), there is a considerable amount of overlap in that region of the ^{13}C spectrum. This

[†] Department of Chemistry.
[‡] Department of Chemical and Fuels Engineering.

10.1021/jp004314k CCC: $20.00
Published on Web 06/21/2001

overlap makes determination of the principal values of the CSTs challenging. The complexity of analyzing this spectrum is reduced by application of the FIREMAT[25,26] experiment (*fi*ve-π *re*plicated *m*agic *a*ngle *t*urning), a two-dimensional (2D) solid state NMR experiment that isolates the sideband pattern associated with each resolvable isotropic chemical shift from the 2D data set.

The use of NMR data to study the inter-ring angle of biphenyl or its derivatives is not a new endeavor. In 1980 Sinton and Pines[27] used ^{1}H multiple quantum NMR to determine the twist angle in the derivative compound 4-cyano-4′-*n*-pentyl-d_{11}-biphenyl. More recent work[28,29] has sought to estimate the twist angle between the ring planes in solid biphenyl and some of its derivatives that are used in liquid crystals. Each of these recent efforts used isotropic chemical shift data, particularly at the C-1 position of the phenyl ring. The approach taken herein uses information provided by the principal values of the CST for all carbons. These experimental values are compared to those predicted by density functional theory. Principal values as opposed to the isotropic shifts establish a very sensitive criterion for characterizing the conformational structure. The predicted CSTs are averaged in several different ways to investigate the nature of the constrained rotational dynamics in the biphenyl crystal.

Methods

Experimental Details. Biphenyl was obtained from Aldrich and was used without further purification. NMR measurements were performed with a double-resonance probe on a Chemagnetics CMX spectrometer operating at 100.62 MHz for ^{13}C and 400.12 MHz for ^{1}H. The ^{1}H pulse width for a $\pi/2$ pulse was 4.2 μs and for ^{13}C it was also 4.2 μs. Chemical shifts are reported relative to TMS via a secondary external reference to the high-frequency peak of adamantane at 38.56 ppm. To enhance signal intensity, all experiments employed cross-polarization (CP).[30] The ^{1}H T_1 for the sample was measured with a saturation recovery pulse sequence to be 545 s. Use of a flip-back pulse enabled a recycle delay of 400 s to be used for optimal signal-to-noise in a given experiment time. Following the T_1 determination the optimal cross-polarization contact time was determined to be 0.9 ms. A high-speed magic angle spinning (MAS) spectrum employing dipolar dephasing identified the signal due to the quaternary carbon. A FIREMAT experiment was performed with a spinning speed of 1920 Hz, an evolution dimension spectral width of 15 360 Hz, and an acquisition dimension of 92 160 Hz. There were 48 points acquired during each rotor period.

Calculations. A series of biphenyl structures was partially optimized with Gaussian98[31] at the B3LYP/D95** level of theory.[32−34] The inter-ring angle was varied from 5°−80° in 5° and 10° increments. The atoms in each ring were planar in all calculations. All optimizations and NMR shielding calculations were performed on isolated molecules. The possible transition states to rotation about the biphenyl linkage include two coplanar rings ($\theta = 0°$) and two perpendicular ring planes ($\theta = 90°$). These respective structures are transition states at this level of theory as each had a single negative eigenvalue in the Hessian. Chemical shifts were calculated for all structures at the GIAO−B3PW91/D95** level of theory.[35−39]

Results

Chemical-Shift Tensors. On the left side of Figure 1 is a plot of the isotropic spectrum constructed from the FIREMAT data. This isotropic spectrum is equivalent to that obtained with high-speed CP/MAS. The degree of overlap for the protonated carbons (the quaternary carbon peak is well resolved) in the isotropic dimension is apparent. The sideband patterns on the right side of Figure 1 are connected to their respective isotropic chemical shift projections. Table 1 reports the principal values determined from the FIREMAT data. An error analysis performed on the biphenyl data estimates the uncertainty in the principal values for C-1 to be 0.4 ppm at the 95% confidence interval and 1.1 ppm for the protonated carbons. The higher uncertainty for the protonated carbon signals reflects several differences between the quaternary carbon signal and the C−H carbon signals. First, residual C−H dipolar interactions lead to larger line widths than in the quaternary carbon signal, leading to modestly lower signal-to-noise in a given spectrum for these peaks than for the quaternary carbon peak. Also, the combination of similar isotropic chemical shifts and larger line widths for these C−H carbon signals leads to partial overlap of the peaks. The TIGER processing utilized in the FIREMAT data analysis achieves resolution at the expense of some signal-to-noise.

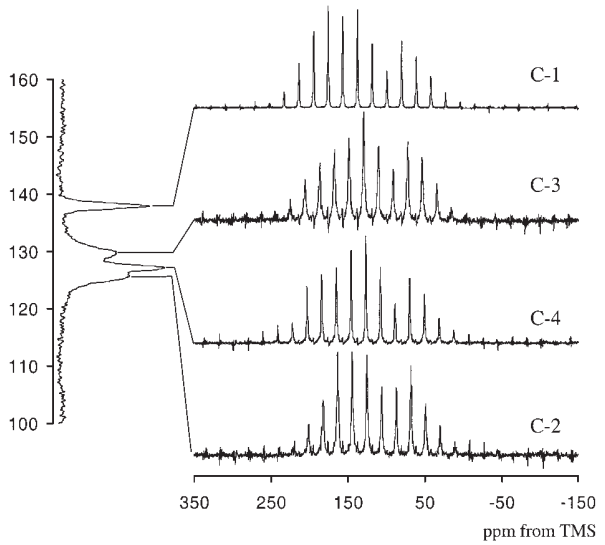

Figure 1. Solid state ^{13}C NMR spectra of biphenyl from the FIREMAT experiment. The isotropic guide spectrum lies on the left with lines drawn to the corresponding isolated sideband patterns on the right that were extracted from the 5π 2D data set by the TIGER processing.

TABLE 1: ^{13}C Chemical Shift Data from the FIREMAT Experiment of Biphenyl

carbon	δ_{11}	δ_{22}	δ_{33}	δ_{iso}	span[a]	acen[b]
C-1	231.7	158.1	24.0	137.9	207.7	30.3
C-2	210.7	142.0	23.7	125.5	187.0	24.8
C-3	229.8	137.5	22.0	129.8	207.8	11.5
C-4	229.0	138.3	14.3	127.2	214.7	16.6

[a] Span $= \delta_{11} - \delta_{33}$. [b] Acentricity $= \delta_{22} - (\delta_{11} + \delta_{33})/2$.

Discussion

Motional Averaging. We ignored intermolecular contributions to the shifts in this work because errors associated with this simplification are usually smaller than the predicted and experimental composite errors. Displacive (translational) effects, well characterized by heat capacity measurements in the lower temperature phases of biphenyl,[13,15,16] are invisible to NMR and are thus ignored. The rotational motion about the phenyl−phenyl linkage present in the biphenyl crystal lattice averages the observed CSTs due to opposing changes in tensor orientations. This sensitive effect can be modeled by theory. It is necessary to resolve these hypothetical averaging processes before com-

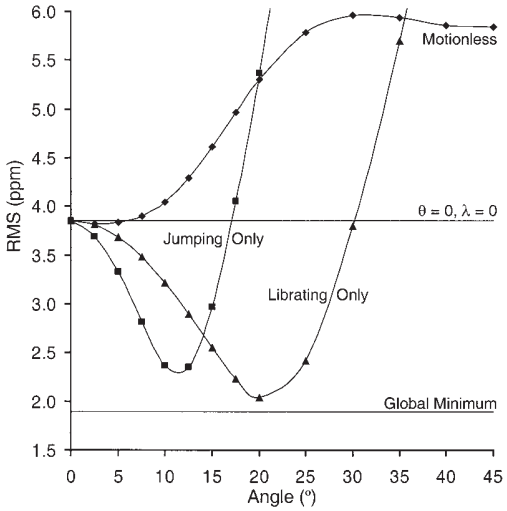

Figure 2. Plot of the rms differences (in ppm) from least squares regressions vs angle (in degrees) for the AB(θ, $\lambda = 0$), AB $\rightleftharpoons$ BA(θ, $\lambda = 0$), and AB $\rightleftharpoons$ BA($\theta = 0$, λ) models. In the case of the librating model, the horizontal axis is the mean libration angle λ not the internal twist angle θ. Each line is labeled with its model. The values for the global minimum and the point AB($\theta = 0$, $\lambda = 0$) are included as horizontal lines for comparison purposes.

pleting the spectral assignments because such rotational perturbations in the crystal could change the observed principal values sufficiently to alter the assignments. The motional averaging (internal jumping and overall molecular libration) involves only rotation of the phenyl rings about biphenyl's long axis. Other librations are neglected because the X-ray crystal work reports that they are smaller than those about the phenyl−phenyl linkage. Hence, all references to motion below refer to constrained rotation about the phenyl−phenyl linkage.

Several models of the molecular dynamics in the crystal were considered. The models are described below in a coordinate system in which two planes (denoted A and B) are separated by a twist angle θ and the phenyl−phenyl linkage is collinear with the intersection of planes A and B. Each phenyl ring must lie sequentially in one of these planes. The letters used to identify the planes denote a molecule's orientation. Thus, AB($\theta = 10°$, $\lambda = 0°$) would specify the first ring in plane A and the second ring in plane B separated by a twist angle of 10°. The second angle, λ, indicates the rms librational angle which is zero in this example. For clarity a given ring is consistently indicated first, thus "AB" and "BA" represent different configurations. Motionless and dynamic models are now discussed.

1. Motionless Model. When internal modes and overall librational solid vibrations give rise to angular distortions with negligible impact on the shift tensor, the motionless model, AB(θ, $\lambda = 0°$), is obtained. In such cases librational motion about the molecular long axis leads to averaging that would be comparable to the relative librational excursions about other molecular axes, e.g., those perpendicular to the long axis. In this relatively motionless case the theoretical predictions are improbable at the model's minimum ($\theta = 5°$, $F = 4.2$), which can be excluded with 98.4% probability relative to the global minimum from the composite model discussed below and become even worse elsewhere, as shown in Figure 2. Thus, the experimental NMR shift tensors fail to support a rigid, motionless model for biphenyl.

2. Dynamic Models. The dynamic models divide into two contributing types discussed separately at first to isolate the specific effects of each. Discussion of a more likely composite follows. First the AB $\rightleftharpoons$ BA(θ, $\lambda = 0°$) model involves two rapidly interconverting structures with overall libration neglected. Second, the AB($\theta = 0°$, $\lambda > 0°$) model involves a planar molecule librating about the mean angular displacement.

2a. Twist or AB $\rightleftharpoons$ BA(θ, $\lambda = 0°$) Model. The molecule "jumps" between the two possible enantiomeric structures for a given value of θ. One cannot predict a priori the time scale of this proposed motion; however, the experimental data exhibit no evidence of slow chemical exchange, thus a fast exchange model is applicable. Under fast chemical exchange each unique carbon occupies one of two spatial positions, one associated with each enantiomer. Rapid exchange between these two positions will result in an averaging of the observed principal values because of the orientational dependence of the CSTs. The calculated carbon tensors are used to simulate the tensors that would be observed in the AB $\rightleftharpoons$ BA(θ, $\lambda > 0$) for a variety of θ values. For each value of θ, the two tensors are averaged. Diagonalization of the averaged tensor yields predicted principal values that are converted to the chemical shift scale by means of a linear regression of the predicted values plotted against the experimental values. By subtracting the experimental shift values from the corresponding predicted average shift values, the difference is used to construct a variance as a function of θ. The best fit of θ comes near $\theta = 25°$ with a variance of 5.51 ppm^2.

2b. Libration or AB $\rightleftharpoons$ BA($\theta = 0°$, $\lambda > 0°$) Model. The second type of motion considered is libration of the whole molecule about the long molecular axis. This motion also alters the observed CST principal values because the tensor orientation with respect to the external magnetic field changes as the molecule librates. In this model the tensors taken directly from the calculation of the planar structure provide the AB structure's tensors. To simulate the librational averaging, a given tensor was averaged over a number of rotated angles that were modulated by a harmonic function. Numerically, the number of modulated angles was increased until the final principal values converged. The effective principal values of each averaged tensor were extracted by symmetrizing then diagonalizing the composite tensor.

This librating model, AB $\rightleftharpoons$ BA($\theta = 0°$, $\lambda > 0°$), exhibits a functional form similar to that of the interconverting model discussed above. The minimal variance (4.07 ppm^2) between predicted and experimental shifts appears at about $\lambda = \pm 15°$ (overall librational excursion of 30°), a value that would render $\langle \lambda^2 \rangle = 225°^2$. This result cannot be statistically distinguished from the former twist dynamic model.

2c. Composite. While it is informative to describe the two modes of rotational averaging—internal twist without libration and libration without internal twist—separately as is done above, the experimental NMR data do not separate these two limiting cases. A more plausible simulation of the possible averaging mechanisms combines the interconverting and overall libration averaging mechanisms. Libration of the two mirror image CSTs from the AB $\rightleftharpoons$ BA model above was simulated as described above in section 2b with integer values for λ from 0° to ±20°. The resulting tensors were averaged, symmetrized, and diagonalized. The single best variance (3.49 ppm^2) from the combination of the two motion types comes with $\theta = 15°$ and $\lambda = \pm 12°$. Figure 3 shows a contour plot of the F surface between predicted and experimental principal values as a function of θ and λ. The minimum lies in a correlated trough.

The motionless model has already been eliminated statistically. The two limiting dynamic models, giving similar statistical data, are both allowable and represent the two axes of the

TABLE 2: Calculated ^{13}C Chemical Shift Data for Selected Calculated Models

model	carbon	δ_{11}	δ_{22}	δ_{33}	δ_{iso}	span[a]	acen[b]
AB($\theta = 5°, \lambda = 0°$)	C-1	220.9	166.6	21.7	136.4	199.1	45.3
	C-2	219.4	141.3	17.8	126.2	201.6	22.7
	C-3	229.1	140.7	19.1	129.6	210.0	16.6
	C-4	225.0	141.0	18.7	128.2	206.3	19.2
AB ⇌ BA($\theta = 25°, \lambda = 0°$)	C-1	228.0	162.4	26.7	139.0	201.3	35.0
	C-2	216.6	137.2	26.2	126.7	190.3	15.8
	C-3	226.6	139.2	19.3	128.4	207.4	16.3
	C-4	231.5	134.7	12.9	126.3	218.5	12.5
AB ⇌ BA($\theta = 0°, \lambda = \pm 15°$)	C-1	228.7	159.2	22.7	136.9	205.9	33.5
	C-2	215.8	140.3	21.3	125.8	194.5	21.7
	C-3	226.7	139.3	23.0	129.7	203.7	14.4
	C-4	233.2	133.1	17.9	128.1	215.3	7.6
AB ⇌ BA($\theta = 15°, \lambda = \pm 12°$)	C-1	228.4	160.5	24.3	137.7	204.1	34.1
	C-2	216.1	139.1	23.3	126.2	192.8	19.4
	C-3	226.6	139.3	21.6	129.1	205.1	15.2
	C-4	232.6	133.8	15.9	127.4	216.7	9.6

[a] Span $= \delta_{11} - \delta_{33}$. [b] Acentricity $= \delta_{22} - (\delta_{11} + \delta_{33})/2$.

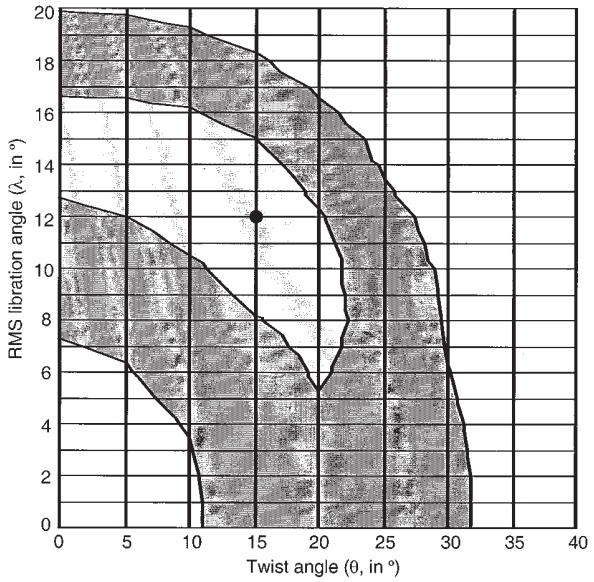

Figure 3. Contour plot of the F values between predicted and measured principal values as a function of θ and λ. The global minimum (12°, 15°) is circled. The contours are drawn at the 68.3% and 94.5% levels. Thus, a point outside the 68.3% contour can be ruled out by an F test relative to minimum with at least 68.3% confidence.

composite model. The jumping component involves a symmetric double-well potential (vide supra) with each enantiomer serving as a local minimum. The transition state between the two enantiomers is likely the planar molecule. This suggests that the repulsions of the *ortho* protons exceed the conjugation energy of the central C−C bond π electron system. The possibility cannot be eliminated that the crystal packing forces could reduce $\langle\theta^2\rangle$ suggested by the descending trend in twist angle from the vapor to liquid to solid phases. Conversely, the low-temperature neutron diffraction structure[14] demonstrates that a distinctive and locked twist angle ($\theta = 10.4°$) exists in a crystalline material. In the AB ⇌ BA($\theta, \lambda > 0°$) model the planar molecule librates in a single harmonic potential with the potential's minimum located at $\langle\lambda\rangle = 0°$, the position at which the statistically averaged molecule is reported in the X-ray structure. The different displacements used in the librational averaging have nonequivalent orientations with respect to the magnetic field.

The motionless and both limiting dynamical models become the same when $\theta = 0°$ and $\lambda = 0°$, giving an untenable F test. Both limiting models show clear improvements over the motionless model especially in the range of $\theta = 25°$ to 30° for AB ⇌ BA($\theta, \lambda = 0°$) and $\lambda = \pm 12°$ to $\pm 16°$ for AB ⇌ BA($\theta = 0, \lambda$). For larger angular deformations (e.g., $\theta \geq 40°$ for or $\lambda \geq |20°|$, respectively) the F value quickly rises for all models relative to the global minimum from the composite model. Hence, one may rule out their consideration.

TABLE 3: Icosohedral Representation Regression Equation Data for Models in Table 2

model	m	b, ppm	R^2	rms, ppm
AB($\theta = 5°, \lambda = 0°$)	−1.066	200.1	0.9955	3.8
AB ⇌ BA($\theta = 25°, \lambda = 0°$)	−0.9892	188.8	0.9980	2.3
AB ⇌ BA($\theta = 0°, \lambda = \pm 7.5°$)	−0.9810	189.0	0.9985	2.0
AB ⇌ BA($\theta = 15°, \lambda = \pm 12°$)	−0.9842	188.9	0.9987	1.9

Spectral Assignment. The assignment of C-1 to the highest frequency peak with an isotropic chemical shift of 137.9 ppm is based on the results of the dipolar dephased experiment. This is also the intuitive assignment: the isotropic shift is fully consistent with substituted quaternary positions in aromatic hydrocarbons, e.g., the quaternary carbons in biphenylene,[20] a molecule with structural similarities to biphenyl. The δ_{22} value for the tensor is also consistent with a substituted aromatic carbon, such as those found in perylene[23] and acenaphthene,[24] which typically lie between 155 and 170 ppm, a frequency range for δ_{22} that is higher than other typical aromatics.

After the averaging effects are considered, the protonated carbon peaks may now be assigned by an algorithm previously described[40] that was modified to use only the principal values of the CST instead of the full tensor. The approach employs the icosohedral representation[41] of the CST and permutes the entire set of possible experimental assignments with the calculated principal values to give a best-fit assignment with the smallest theoretical/experimental variance. Application of an F test at a given confidence level then determines statistically whether the best fit is distinguishable from alternative assignments. While C-1 is already unambiguously assigned, it is confirmed by the above procedure, thereby lending support to this processing of the spectral data.

The second column of Table 2 contains the best assignment of the calculated tensors to molecular carbon positions for all three models. Also included in Table 2 is the calculated chemical-shift data at the values of θ and λ that yield the lowest variance for that model. In all models presented in this work, the change in neither θ nor λ ever altered the best assignment. In the motionless model the C-1 assignment at all angles is correct to at least the 99.9% confidence level relative to the

global minimum. In the averaged cases, for all twist angles up to and including 35°, the C-1 carbon assignment is preferred over any other possible assignment for that carbon with at least 99.9% confidence relative to the global minimum. With C-1 unambiguously assigned on the basis of the dipolar dephased experiment as well as the assignment procedure, it may be removed from the pool of possibilities to emphasize the three protonated carbons in the subsequent analysis. Even when focusing on the CH carbons, the best assignment of the three C−H peaks is identical to the above procedure and is shown in Table 2. The graph in Figure 2 shows that either averaging model fits experimental data better than the AB model. The rms differences for either averaging case are comparable to those found in other work in this laboratory for aromatic hydrocarbons.[20,22,23] All of the chemical shift assignments are consistent with previous work.[28,29]

Either averaging model clearly provides a better fit to the experimental data than the AB($\theta = 0°$, $\lambda = 0°$) model. If the crystal system exhibited static disorder (i.e., nonexchanging distinct molecular conformations at equivalent crystallographic sites), there would be no motion, thus there would be no averaging of the tensors. There would instead be more lines in the NMR spectrum (not necessarily resolved) as different chemical environments due to the disorder would lead to modestly different chemical shifts. The solid state NMR data therefore suggest that the biphenyl crystal system exhibits motional averaging instead of static disorder. Unfortunately, the mechanism of the averaging cannot be determined unequivocally from NMR data. The two-ring motion is estimated to be composed of 15° from internal twist and ±12° from librational excursions in room temperature crystals. Lower temperature data likely could provide further detail of these averaging processes.

Acknowledgment. This work was funded by Basic Energy Sciences, U.S. Department of Energy, through grant DE-FG03-94ER14452. Computer resources were provided by the Center for High Performance Computing at the University of Utah and also by the HHMI Undergraduate Biological Sciences Education Program Grant 71196-552201 at Washington & Jefferson College. R.J.I. was supported by Los Alamos National Lab under contract number E90240017-3L. We thank Don W. Alderman for many helpful and insightful discussions in the course of this work.

References and Notes

(1) Bastiansen, O. *Acta Chem. Scand.* **1949**, *3*, 408−414.
(2) Almenningen, A.; Bastiansen, O.; Fernholt, L.; Cyvin, B. N.; Cyvin, S. J.; Samdal, S. *J. Mol. Struct.* **1985**, *128*, 59−76.
(3) Suzuki, H. *Bull. Chem. Soc. Jpn.* **1959**, *32*, 1340−1350.
(4) Eaton, V. J.; Steele, D. *J. Chem. Soc., Faraday Trans. 2* **1973**, 1601.
(5) Clark, G. L.; Pickett, L. W. *Proc. Natl. Acad. Sci. U.S.A.* **1930**, *16*, 20−27.
(6) Clark, G. L.; Pickett, L. W. *J. Am. Chem. Soc.* **1931**, *53*, 167−177.
(7) Dhar, J. *Indian J. Phys.* **1932**, *7*, 43−60.
(8) Robertson, G. B. *Nature (London)* **1961**, *191*, 593−594.
(9) Trotter, J. *Acta Crystallogr.* **1961**, *14*, 1135−1140.
(10) Hargreaves, A.; Rizvi, S. H. *Acta Crystallogr.* **1962**, *15*, 365−373.
(11) Charbonneau, G.; Delugard, Y. *Acta Crystallogr.* **1976**, *B32*, 1420−1423.
(12) Charbonneau, G.; Delugard, Y. *Acta Crystallogr.* **1977**, *B33*, 1586−1588.
(13) Atake, T.; Chihara, H. *Solid State Commun.* **1980**, *35*, 131−134.
(14) Cailleau, H.; Baudour, J. L. Zeyen, C. M. *Acta Crystallogr.* **1979**, *B35*, 426−432.
(15) Saito, K.; Atake, T.; Chihara, H. *J. Chem. Thermodyn.* **1986**, *18*, 407−414.
(16) Saito, K.; Atake, T.; Chihara, H. *Bull. Chem. Soc. Jpn.* **1988**, *61*, 2327−2336.
(17) Badour, J. L.; Charbonneau, G. P. *Acta Crystallogr.* **1974**, *B30*, 1379.
(18) Delugeard, Y.; Desuche, J.; Baudour, J. L. *Acta Crystallogr.* **1976**, *B32*, 150−154.
(19) Saito, K.; Atake, T.; Hideaki, C. *J. Chem. Thermodyn.* **1985**, *17*, 539−548.
(20) Barich, D. H.; Orendt, A. M.; Pugmire, R. J.; Grant, D. M. *J. Phys. Chem. A* **2000**, *104*, 8290−8295.
(21) Orendt, A. M.; Facelli, J. C.; Bai, S.; Rai, A.; Gossett, M.; Scott, L. T.; Boerio-Goates, J.; Pugmire, R. J.; Grant, D. M. *J. Phys. Chem. A* **2000**, *104*, 149−155.
(22) Iuliucci, R. J.; Phung, C. G.; Facelli, J. C.; Grant, D. M. *J. Am. Chem. Soc.* **1998**, *120*, 9305−9311.
(23) Iuliucci, R. J.; Phung, C. G.; Facelli, J. C.; Grant, D. M. *J. Am. Chem. Soc.* **1996**, *118*, 4880−4888.
(24) Iuliucci, R. J.; Facelli, J. C.; Alderman, D. W.; Grant, D. M. *J. Am. Chem. Soc.* **1995**, *117*, 2336−2343.
(25) McGeorge, G.; Hu, J. Z.; Mayne, C. L.; Alderman, D. W.; Pugmire, R. J.; Grant, D. M. *J. Magn. Reson.* **1997**, *129*, 134−144.
(26) Alderman, D. W.; McGeorge, G.; Hu, J. Z.; Pugmire, R. J.; Grant, D. M. *Mol. Phys.* **1998**, *95*, 1113−1126.
(27) Sinton, S.; Pines, A. *Chem. Phys. Lett.* **1980**, *76*, 263−267.
(28) Ando, S.; Hironaka, T.; Kurosu, H.; Ando, I. *Magn. Reson. Chem.* **2000**, *38*, 241−250.
(29) Chippendale, A. M.; Aujla, R. S.; Harris, R. K.; Packer, K. J.; Purser, S. *Magn. Reson. Chem.* **1986**, *24*, 81−88.
(30) Pines, A.; Gibby, M. G.; Waugh, J. S. *J. Chem. Phys.* **1973**, *59*, 569−590.
(31) Frisch, M. J.; Trucks, G. W.; Schlegel, H. B.; Scuseria, G. E.; Robb, M. A.; Cheeseman, J. R.; Zakrzewski, V. G.; Montgomery, J. A., Jr.; Stratmann, R. E.; Burant, J. C.; Dapprich, S.; Millam, J. M.; Daniels, A. D.; Kudin, K. N.; Strain, M. C.; Farkas, O.; Tomasi, J.; Barone, V.; Cossi, M.; Cammi, R.; Mennucci, B.; Pomelli, C.; Adamo, C.; Clifford, S.; Ochterski, J.; Petersson, G. A.; Ayala, P. Y.; Cui, Q.; Morokuma, K.; Malick, D. K.; Rabuck, A. D.; Raghavachari, K.; Foresman, J. B.; Cioslowski, J.; Ortiz, J. V.; Baboul, A. G.; Stefanov, B. B.; Liu, G.; Liashenko, A.; Piskorz, P.; Komaromi, I.; Gomperts, R.; Martin, R. L.; Fox, D. J.; Keith, T.; Al-Laham, M. A.; Peng, C. Y.; Nanayakkara, A.; Gonzalez, C.; Challacombe, M.; Gill, P. M. W.; Johnson, B.; Chen, W.; Wong, M. W.; Andres, J. L.; Gonzalez, C.; Head-Gordon, M.; Replogle, E. S.; Pople, J. A. *Gaussian 98* (Revision A.7); Gaussian, Inc.: Pittsburgh, PA, 1998.
(32) Becke, A. D. *J. Chem. Phys.* **1993**, *98*, 5648−5652.
(33) Lee, C.; Yang, W.; Parr, R. G. *Phys. Rev. B* **1988**, *37*, 785−789.
(34) Dunning, T. H., Jr. *J. Chem. Phys.* **1989**, *90*, 1007−1023.
(35) Perdew, J. P.; Wang, Y. *Phys. Rev. B* **1992**, *45*, 13244−13249.
(36) Ditchfield, R. *Mol. Phys.* **1974**, *27*, 789−807.
(37) Wolinski, K.; Hinton, J. F.; Pulay, P. *J. Am. Chem. Soc.* **1990**, *112*, 8251−8260.
(38) Cheeseman, J. R.; Trucks, G. W.; Keith, T. A.; Frisch, M. J. *J. Chem. Phys.* **1996**, *104*, 5497−5509.
(39) Rauhut, G.; Puyear, S.; Wolinski, K.; Pulay, P. *J. Phys. Chem.* **1996**, *100*, 6310−6316.
(40) Liu, F.; Phung, C. G.; Alderman, D. W.; Grant, D. M. *J. Magn. Reson. A* **1996**, *120*, 231−241.
(41) Alderman, D. W.; Sherwood, M. H.; Grant, D. M. *J. Magn. Reson.* **1993**, *101*, 188−197.